SAND2013-3920C

Net Versus Gross Erosion of High-Z Materials in the Divertor of DIII-D

D.L. Rudakov[a,*], P.C. Stangeby[b], W.R. Wampler[c], J.N. Brooks[d], N.H. Brooks[e], J.D. Elder[b], A. Hassanein[d], A.W. Leonard[e], A.G. McLean[f], R.A. Moyer[a], T. Sizyuk[d], J.G. Watkins[g], and C.P.C. Wong[e]

*E-mail: rudakov@fusion.gat.com

[a]*University of California San Diego, 9500 Gilman Dr., La Jolla, California 92093-0417, USA*
[b]*University of Toronto Institute for Aerospace Studies, Toronto, M3H 5T6, Canada*
[c]*Sandia National Laboratories, Albuquerque, New Mexico 87185, USA*
[d]*Purdue University, West Lafayette, Indiana, USA*
[e]*General Atomics, PO Box 85608, San Diego, California 92186-5608, USA*
[f]*Lawrence Livermore National Laboratory, Livermore, California 94550, USA*
[g]*Sandia National Laboratories, Livermore, California 94551, USA*

Abstract. A substantial reduction of net compared to gross erosion of molybdenum and tungsten was observed in experiments conducted in the lower divertor of DIII-D using the Divertor Material Evaluation System (DiMES). Post-exposure net erosion of Mo and W films was measured by Rutherford backscattering (RBS) yielding net erosion rates of 0.4 – 0.7 nm/s for Mo and ~0.14 nm/s for W. Gross erosion was estimated using RBS on a 1 mm diameter sample, where re-deposition is negligible. Net erosion on a 1 cm diameter sample was reduced compared to gross erosion by factors of ~2 for Mo and ~3 for W. The experiment was modeled with the REDEP/WBC erosion/redeposition code package coupled to the ITMC-DYN mixed-material code, with plasma conditions supplied by the OEDGE code with input from divertor Langmuir probes. The code-calculated net/gross erosion rate ratios of 0.46 for Mo and 0.29 for W are in agreement with the experiment.

PACS numbers: 52.40.Hf, 52.55.Fa, 52.55.Rk

1. Introduction

Net erosion of high-Z plasma-facing components (PFCs) in a tokamak is expected to be reduced by local redeposition due to sputtered atom/ion collisions with the impinging plasma and Lorentz forces [1]. In earlier experiments on ASDEX Upgrade [2] and DIII-D [3,4], samples of tungsten, molybdenum and vanadium were exposed to divertor plasma, and post-experiment analysis found redeposited material mostly within a few mm from the samples, supporting the local redeposition picture. A reduction of net compared to gross erosion has

been demonstrated for tungsten in ASDEX Upgrade [5]. However, in Alcator C-Mod the measured campaign-integrated peak net erosion of Mo divertor tiles was found to be ~10X higher than that computed using the REDEP/WBC code package, while the *gross* erosion predicted by the code was a reasonable match to MoI influx data [6]. The experiments at DIII-D reported here were aimed at measuring both net and gross erosion of molybdenum and tungsten under short-exposure, stable, well-diagnosed plasma conditions allowing a more accurate comparison with the modeling. Experiments with Mo have been reported earlier [7,8]; here we will present a brief overview for completeness. Results for W have not been previously reported. We also report a novel non-spectroscopic method for measuring the gross erosion rate, based on post-experiment ion bean analysis (IBA) analysis of the net erosion of a sample that is smaller than the characteristic redeposition lengths of the sputtered atoms for the plasma conditions involved (see Sections 3, 4).

2. Experimental approach

Three experiments with Mo and one experiment with W were conducted in the lower divertor of the DIII-D tokamak [9]. Molybdenum was initially chosen over tungsten for better known inverse photon efficiency coefficients, S/XB, and also for better comparison with Alcator C-Mod results. In order for net erosion to be measurable by IBA, thin coatings of Mo on a silicon substrate were used. All samples featured a 1 cm diameter 15 – 25 nm thick film of Mo or W in the center, while in the latest experiment with Mo and the one with W there was also a 1 mm spot for gross erosion measurement (marked by an arrow in Fig. 1(a)). In those two experiments, the metallic films were deposited on a Si disc ~23 mm in diameter over a carbon inter-layer ~300 nm thick to prevent exposure of Si to plasma. Films were deposited in a magnetron sputter deposition system at Sandia National Laboratories in Albuquerque NM. All samples were pre-characterized by IBA before the exposures. For the exposures, the samples were installed in graphite casings and inserted in the lower divertor of DIII-D using the Divertor Material Evaluation System (DiMES) manipulator [10]. During the exposures, the top surface of the DiMES probe with deposited metal films was level with the divertor tile surfaces within 0.1-0.2 mm.

All experiments were performed in L-mode deuterium discharges, in a Lower Single Null (LSN) magnetic configuration. Figure 1(b) shows a poloidal cross-section of DIII-D with a typical equilibrium last closed flux surface (LCFS) and the diagnostic arrangement. In the exposure discharges, the outer strike point (OSP) was kept off DiMES sample during the

plasma current ramp-up and ramp-down. Once stable conditions were achieved around 1 s into the discharge, the OSP was moved to near the inboard edge of the samples and dwelled there for 3 – 4 s in each exposure discharge. Before each exposure, a number of characterization shots with OSP sweeps were taken in order to obtain plasma density and temperature profiles from the floor Langmuir probes and divertor Thomson scattering (DTS).

The samples were imaged by an absolutely calibrated digital CMOS camera in order to get a spectroscopic estimate of the gross erosion. For Mo, the S/XB coefficient measured on PISCES by Nishijima, et al. [11] was used. In the first experiment with Mo, a MoI filter centered around 390 nm and having a bandwidth of ~10 nm was used. The 10 nm bandwidth passed several non-MoI lines including a few CII lines identified using a high resolution MDS spectrometer [12]. Figure 1(c) shows an image of the sample taken with this filter. The bright band of light inboard of the sample is entirely due to non-Mo lines. In ordert to reduce the error bars, in the next two experiments a 1 nm bandwidth filter centered on the MoI line at 386 nm was used. The MDS spectrometer measured no emission in this 1 nm passband other than the MoI line. Finally, in the W experiment, a WI filter centered on 400.0 mn with a 3 nm bandwidth was used.

Net erosion of Mo and W was measured by comparing the metal layer thickness measured by Rutherford backscattering (RBS) before and after the exposure [8]. The distribution of the metals redeposited on the graphite surface surrounding the samples was also measured by RBS.

3. Experimental results

The results from the four experiments are summarized in Table 1. Results for Mo are discussed in detail in Refs. [7,8]. The measured net erosion rates varied between 0.4 – 0.7 nm/s, most likely because of the difference in the local plasma parameters near the samples. The spectroscopic estimate of the gross erosion rate made for the first experiment had large error bars (± 60%), mostly due to CII light leakage through the filter. In the next two experiments the uncertainty was reduced to be within ± 40%. In the third experiment, a non-spectroscopic measurement of the gross erosion from the 1 mm spot gave a rate of 1.38 nm/s. The experimental ratio of net/gross erosion rates for Mo was therefore within 0.3 – 0.5, in reasonable agreement with modeling (Section 4).

The redeposition pattern of Mo on the surface of the graphite holder measured after the first experiment was qualitatively as expected. Mo deposits were concentrated near the Mo sample edge, with an e-folding length of ~2 mm. The concentration of the deposited Mo was

a factor of 8–10 larger on the downstream side of the sample compared to the upstream side. An initially surprising result was that the total amount of Mo found on the holder was only ~19% of the net amount of Mo eroded from the sample. However, this result turned out to be in reasonable agreement with modeling (Section 4).

Tungsten, being the most fusion relevant high-Z PFC material, was a logical next step after Mo. The primary goal of the W exposure was to confirm the expected stronger reduction of net/gross erosion compared to Mo and to benchmark the modeling codes for W. The secondary goal was to compare spectroscopic and non-spectroscopic measurements of the gross erosion rate and derive an experimental value of the S/XB coefficient.

Figure 2 shows radial profiles (versus the distance from OSP) of electron density and temperature measured by the floor Langmuir probes in a setup discharge for W exposure featuring an OSP sweep. The location of the 1 cm W sample with respect to the OSP during the following exposure discharges is marked by the vertical dashed lines. Density and temperature are essentially uniform over the sample surface at $T_e \approx 37$ eV, $n_e \approx 1.2$ x10^{19} m^{-3}. The actual sample exposure was performed in four plasma discharges for a total of ~16 seconds. Three of the discharges had good OSP position control, and in one the OSP drifted away from DiMES by a few cm during the exposure, making effective plasma temperature and density at the sample location 20-30 % lower.

During the exposure, the W sample was imaged by the CMOS camera with WI filter centered at 400.0 nm. However, the wide pass band of the filter, ~3 nm, led to signal contamination by CII, HI (the 397 nm D Balmer line), and He I (the 402.6 nm multiplet) light. Unfortunately, the contamination was so strong that it made camera data useless for the estimates of the gross erosion rate of W. Therefore, the secondary goal of the experiment could not be accomplished.

After the exposure, the sample was analyzed by RBS with 2 MeV ^{4}He beam [8]. RBS measures the number of atoms per unit area. Measured areal densities can be expressed as a physical thickness by dividing by the standard atomic volume density of metallic W, 0.63x10^{23} atoms/cm^3. The W areal density on the 1 mm spot before the exposure was 9.34 x10^{16} atoms/cm^2 and after the exposure 4.6 x10^{16} atoms/cm^2, corresponding to a net erosion of 4.8 (±0.2) x10^{16} atoms/cm^2 or 7.6 nm. Comparison of pre- and post-exposure RBS measurements is presented in Fig. 3 for two scans across the sample surface in toroidal (B_T) and radial directions. The results are plotted versus distance from the center of the sample. Net erosion of W from the 1 cm spot (occupying the area between -5 and 5 mm) is illustrated in Fig. 3(a) (note the expanded vertical scale), while Fig. 3(a) shows redeposition of W on the

surrounding carbon-coated area (note the semi-log vertical scale). The isolated peak at -9 mm on the toroidal scan in Fig. 3(b) corresponds to the 1 mm W spot. The dashed lines show fits to an exponential for the inboard and outboard sides of the radial scan and for the downstream side of the toroidal scan.

It is evident that the net erosion of W from the 1 cm spot is greater near the edge of the sample compared to the center, consistent with reduction of net erosion by redeposition. Furthermore, in the toroidal direction the erosion is the largest near the upstream edge, and in the radial direction it is the largest at the inboard edge (both corresponding to negative distances from the center in Fig. 3). Both of these effects are expected, since the plasma flow tends to push the eroded W away from the upstream edge reducing local redeposition there, while the inboard edge is closest to the OSP, and T_e and n_e are slightly larger there than over the rest of the sample, causing higher erosion rate. The net erosion at the center of the 10 mm spot, obtained from the pre-exposure value at the center minus the average of the post-exposure values at the center and ± 1 mm from the center for both scans, is 1.36 (±0.2) $x10^{16}$ atoms/cm^2 or 2.16 nm. The total quantity of W eroded from the film can be estimated by integrating the areal density over the radius, using the average of the measured values at each radius, and subtracting this from the amount before the exposure. This gives 2.3 (±0.3) $x10^{16}$ atoms; dividing by the area of the film gives an average erosion of 1.8 (±0.2) $x10^{16}$ atoms/cm^2 (2.86 nm), which is 32% larger than the erosion at the center.

Tungsten deposition is strongest on the downstream side of the sample, as expected. Deposition cannot be reliably determined on the upstream side of the toroidal scan due to interference from the 1 mm spot at -9 mm, but the W coverage on this side is not too different from the radial scan at each end away from the 1 mm spot. The e-folding lengths for the three fits are 2.0 mm for the outboard radial, 2.5 mm for the inboard radial, and 3.0 mm for the downstream toroidal sectors. The total quantity of deposited W can be estimated by integrating the measured W coverage over the radius, assuming a uniform radial dependence within each quadrant, and approximating the coverage on the upstream toroidal sector as the average of the coverage on two radial scans. This gives the amount of W deposited on the disk (i.e., between 5 mm < R < 12 mm) as 0.62 (±0.06) $x10^{16}$ atoms. The amount of W that would be deposited at greater radii, R > 12mm, is estimated to be about 0.1 $x10^{16}$ atoms by extrapolating the exponential dependence of coverage over the radius. Comparing the amount of W deposited on the sample to the quantity lost from the original film, the fraction of eroded W which has been redeposited on the sample is 27±3 % with only another 4% deposited at

greater radii, assuming a continuing exponential decrease with radius. This is qualitatively similar to the result found previously for Mo, as mentioned earlier in this section.

Since the 1 mm spot is smaller than the characteristic length for redeposition (2 to 3 mm), there should not be significant redeposition of the eroded W back onto this spot (which is confirmed by modeling, see Section 4). Therefore the amount of erosion measured from this spot should approximate the "gross" erosion, without redeposition. Conversely, the 10 mm spot size is roughly comparable to characteristic transport/redeposition lengths; thus involving much higher redeposition and less net erosion than the small spot. Taking the erosion from the 1 mm spot as the "gross" value and erosion from the center of the 10 mm spot as the "net" value, the ratio net/gross = 0.28, i.e., 72% of eroded tungsten is locally redeposited at the center of the 10 mm spot.

4. Modeling

Sputtering and transport of Mo and W from the DiMES samples were modeled with the REDEP/WBC [13,14] erosion/redeposition code package coupled to the ITMC-DYN [15-17] mixed-material evolution/response code, part of the HEIGHTS package [18], with plasma conditions supplied by the OEDGE code with Langmuir probe data input [19]. As described in e.g. [13,14] WBC computes the 3-D, sub-gyro-orbit, fully-kinetic motion of sputtered atoms/ions, subject to the Lorentz force, and velocity-changing and charge-changing collisions with the plasma. Major new simulation capability involves the metal/carbon mixed-material evolution and re-sputtering of metals deposited in the carbon divertor surface, per coupled REDEP/ITMC-DYN calculations, as described in [20]. Focus of the initial modeling effort was on the first Mo experiment. Later the modeling was repeated for W experiment, albeit not in a fully self-consistent way for lack of resources.

Modeling inputs include deuterium plasma with 1% carbon, with nominal at-probe sheath/ plasma boundary conditions measured by the Langmuir probes, sound speed flow at the solid surface, and measured magnetic field components. The BHI-3D sheath code [21] was used to verify WBC models for the dual structure, magnetic + Debye sheath, including incident carbon ion impingement energy/angle for the studied DIII-D conditions.

The REDEP simulations show a high Mo redeposition fraction (54%) on the 1 cm Mo spot and a consequent ratio of 0.46 for net/gross erosion. The initially surprising result that only 19% of the Mo removed from the 1 cm sample was found on the 5 cm DiMES graphite head is seen in ITMC-DYN modeling to be due to fast saturation of the Mo in C and

subsequent re-sputtering. The predicted fraction of net eroded Mo redepositing on the DiMES head is 13%, which compares well with the IBA measured 19%. The rest of the eroded Mo is predicted to deposit in the divertor away from DiMES head, resulting in a ~100% overall Mo redeposition on the divertor surfaces (including the DiMES head) with essentially zero core plasma Mo contamination. Although experiments 2 and 3 were not simulated in as much detail, initial modeling indicates similar trends. As discussed in [6] however, there remains an unexplained code/data discrepancy in upstream/downstream transport of sputtered Mo, with the data showing less upstream transport.

REDEP/WBC modeling of W erosion was performed using plasma conditions supplied by OEDGE based on Langmuir probe data of Fig.2. C on W sputtering and W self-sputtering yields were given by ITMC-DYN code calculations for a pure tungsten spot; no D^+ sputtering was predicted. Analysis of W transport to/from the carbon portion of DiMES probe was performed using the previous WBC/ITMC-DYN coupled results for Mo, extrapolated (mass-adjusted) to W. Modeling results show good agreement with RBS measurements. Net W erosion from the 1 cm spot was calculated at 1.5×10^{16} atoms/cm^2 (versus 1.8×10^{16} from RBS), and predicted net erosion from the 1 mm spot was 4.5×10^{16} atoms/cm^2 (versus 4.8×10^{16} from RBS). Calculated redeposition fractions on the 1 cm and 1 mm spots were respectively 0.72 and 0.03, confirming that the net erosion on the smaller spot is approximately equal to gross erosion. The calculated ratio of net erosion from the 1 cm spot to net erosion from the 1 mm spot (approximately equal to net/gross erosion ratio) was 0.33, likewise in good agreement with the experimental value of 0.28.

5. Summary and future plans

For a specific divertor plasma condition (attached L-mode, low density, relatively high T_e) the measured ratio of net to gross erosion for Mo and W was found to agree well with code modeling. The ITMC-DYN/REDEP/WBC simulations show high redeposition fraction (54% for Mo and 72% for W) on the 1 cm diameter sample, in good agreement with the post-exposure RBS data. Furthermore, the simulations predict essentially complete (~100%) redeposition on the divertor generally. Such high-Z sputtered material transport behavior has positive implications for the ITER tungsten divertor, tending to support predictions of low net erosion and core plasma contamination.

The sputtered high-Z material that does not promptly redeposit on the 1 cm sample apparently travels only a short distance before redeposition adjacent to the edge of the Mo

sample, as evidenced by the rapidly decaying profiles in Fig. 4(b). However, there is also longer range transport of some ions caused by re-sputtering from the DiMES carbon surface, involving mixed materials effects including a high sputtering rate due to shallow deposition of the metals and reduced binding energy of metals with carbon compared to that with a high-Z metallic surface.

A new, non-spectroscopic method for measuring gross erosion rates has been demonstrated, based on post-experiment surface analysis measurement of the net erosion experienced by a very small sample where gross erosion is close to net erosion. Such a method makes optimum use of the removable DiMES facility, and provides confirmation of the spectroscopic method which is subject to a number of uncertainties, including the values of the S/XB ratio. The non-spectroscopic method provides a means of calibrating S/XB for general tokamak use.

In future experiments exposure of W samples to "stronger" plasma conditions with higher n_e and T_e is planned, while staying in L-mode for the ease of interpretation and comparison with modeling. Under "stronger" conditions, gross erosion is expected to increase, improving the potential for spectroscopic measurements and calculating the S/XB coefficient. A narrower pass band WI filter will be used to prevent signal contamination by non-W light. It is also proposed to deposit a W sample over a Mo inter-layer in order to study redeposition in a different mixed material environment.

Acknowledgment

This work was supported in part by the US Department of Energy under DE-FG02-07ER54917, DE-FC02-04ER56498, DE-FC02-04ER54698, and DE-AC52-07NA27344 and supported grant from the National Sciences and Engineering Research Council of Canada. Sandia National Laboratories is a multi-program laboratory managed and operated by Sandia Corporation, a wholly owned subsidiary of Lockheed Martin Corporation, for the U.S. Department of Energy's National Nuclear Security Administration under contract DE-AC04-94AL85000.

References

[1] BROOKS, J.N., Nuclear Tech./Fus. **4** (1983) 33.

[2] NAUJOKS, D., *et al.*, J. Nucl. Mater. **210** (1994) 43.

[3] BASTASZ, R., *et al.*, J. Nucl. Mater. **220-222** (1995) 310.

[4] WAMPLER, W.R., *et al.*, J. Nucl. Mater. **233-237** (1996) 791.

[5] KRIEGER, K., *et al.*, J. Nucl. Mater. **266-269** (1999) 207.

[6] BROOKS, J.N., *et al.*, J. Nucl. Mater. **415** (2011) S112.

[7] STANGEBY, P.C., *et al.*, "An experimental comparison of gross and net erosion of Mo in the DIII-D divertor," 20th Intl. Conf. on Plasma-Surface Interactions in Controlled Fusion Devices, Aachen, Germany, 2012 to be published in the J. Nucl. Mater.

[8] WAMPLER, W.R., *et al.*, "Measurements of net erosion and redeposition of molybdenum in DIII-D," 20th Intl. Conf. on Plasma-Surface Interactions in Controlled Fusion Devices, Aachen, Germany, 2012 to be published in the J. Nucl. Mater.

[9] LUXON, J.L., Nucl. Fusion **42** (2002) 614.

[10] WONG, C.P.C., *et al.,* J. Nucl. Mater. **258–263** (1998) 433.

[11] NISHIJIMA, D., *et al.*, J. Phys. B: At. Mol. Opt. Phys. **43** (2010) 225701.

[12] BROOKS, N.H., *et al.,* Rev. Sci. Instrum. **63** (1992) 5167.

[13] BROOKS, J.N., Phys. Fluids **8** (1990) 1858.

[14] BROOKS, J.N., WHYTE, D.G., Nucl. Fusion **39** (1999) 525.

[15] HASSANEIN, A., SMITH, D.L., Nucl. Instr. and Meth. B **13** (1986) 225.

[16] SIZYUK, T., HASSANEIN, A., J. Nucl. Mater. **404** (2010) 60-67.

[17] SIZYUK, T., HASSANEIN, A., "Dynamic evolution of plasma facing surfaces in NSTX: impact of impurities and substrate composition on fuel recycling," 20th Intl. Conf. on Plasma-Surface Interactions in Controlled Fusion Devices, Aachen, Germany, 2012 to be published in the J. Nucl. Mater.

[18] HASSANEIN, A., SIZYUK, V., MILOSHEVSKY, G., SIZYUK, T., "Can tokamaks PFC survive a single event of any plasma instabilities?," 20th Intl. Conf. on Plasma-Surface Interactions in Controlled Fusion Devices, Aachen, Germany, 2012 to be published in the J. Nucl. Mater.

[19] STANGEBY, P.C., *et al.,* J. Nucl. Mater. **313–316** (2003) 883.

[20] BROOKS, J.N., *et al.*, "Advanced simulation of mixed-material erosion/evolution and application to Mo, C, Be, W containing plasma facing components," 20th Intl. Conf. on Plasma-Surface Interactions in Controlled Fusion Devices, Aachen, Germany, 2012 to be published in the J. Nucl. Mater.

[21] BROOKS, J.N., NAJUOKS, D., Phys. Plasmas **7** (2000) 2565.

Expt #	Element	Expo-sure time (s)	Te (eV)	n_e ($x10^{19}m^{-3}$)	Net erosion rate (nm/s)	Gross erosion rate (nm/s)	Net/gross erosion experiment	Net/gross erosion model
1	Mo	28	30±8 (LP and DTS)	0.8±0.2 (DTS)	0.42	2.39±1.4*	0.18±60%	0.46
2	Mo	12	22±5 (DTS)	1.4±0.2 (DTS)	0.5	1.45±0.6*	0.34±40%	
3	Mo	4	40 (LP) 25±7 (DTS)	1.2 (LP) 1.1±0.2 (DTS)	0.73	2.45±1.0* 1.38**	0.30±40% 0.53±12%	
4	W	16	35 (LP)	1.2 (LP)	0.14	0.48**	0.29	0.33

LP = Langmuir probes, DTS = Divertor Thomson scattering

* spectroscopic, ** non-spectroscopic (RBS of 1 mm sample)

Table 1: Summary of the experimental and modeling results for 4 experiments conducted in DIII-D. No probe data were available for experiment #2. Detailed modeling of experiments #3 and #4 was not performed.

Figure captions

Fig. 1. Pre-exposure photograph of the DiMES holder with 1 cm and 1 mm W samples (a); experimental setup showing LCFS, DiMES, and views of CMOS camera and MDS (b); image of the sample taken during the 1st experiment by the camera with MoI 390 nm filter (c).

Fig. 2. Radial profiles (versus the distance from OSP) of electron density and temperature measured by the floor Langmuir probes in a setup discharge for W exposure featuring an OSP sweep. Location of the W sample with respect to OSP is marked by the vertical dashed lines.

Fig. 3. Pre- and post-exposure RBS measurements of W coverage on the sample

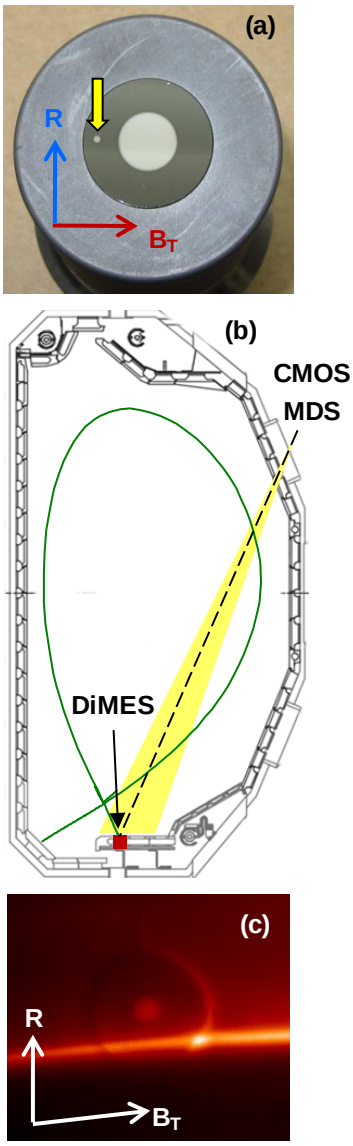

Fig. 1. Pre-exposure photograph of the DiMES holder with 1 cm and 1 mm W samples (a); experimental setup showing LCFS, DiMES, and views of CMOS camera and MDS (b); image of the sample taken during the 1st experiment by the camera with MoI 390 nm filter (c).

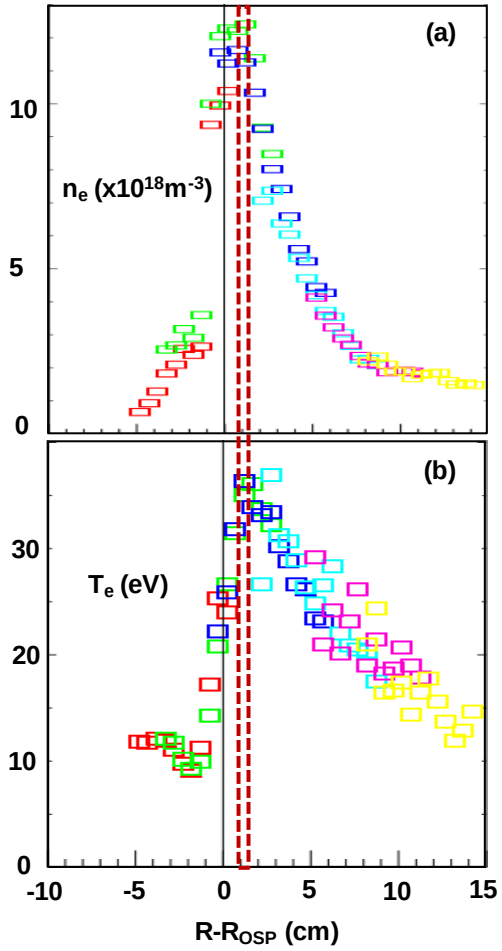

Fig. 2. Radial profiles (versus the distance from OSP) of electron density and temperature measured by the floor Langmuir probes in a setup discharge for W exposure featuring an OSP sweep. Location of the W sample with respect to OSP is marked by the vertical dashed lines.

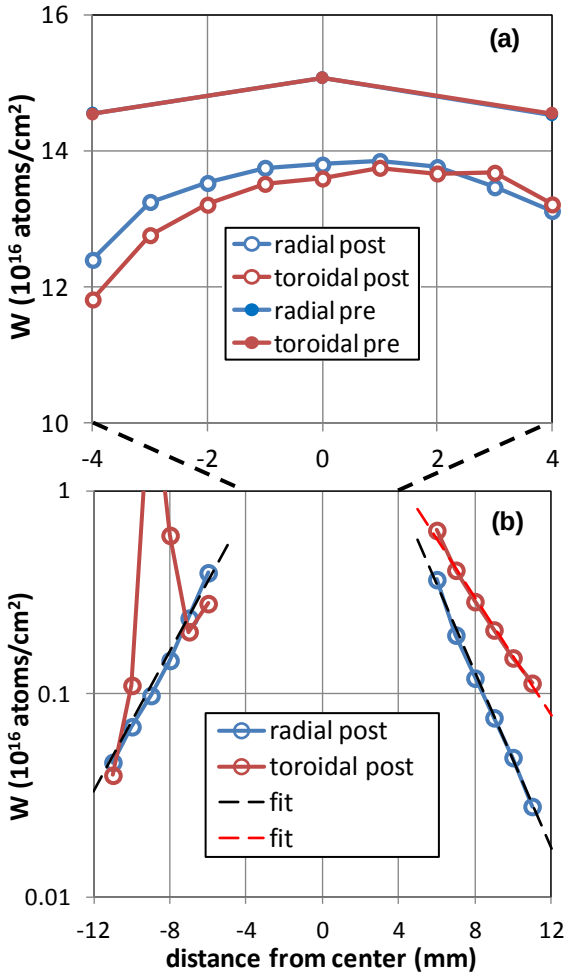

Fig. 3. Pre- and post-exposure RBS measurements of W coverage on the sample